# Decentralized Operation of Interdependent Power Distribution Network and District Heating Network: A Market-Driven Approach

Yang Cao, *Student Member, IEEE*, Wei Wei, *Senior Member, IEEE*, Lei Wu, *Senior Member, IEEE*, Shengwei Mei, *Fellow, IEEE*, Mohammad Shahidehpour, *Fellow, IEEE*, and Zhiyi Li, *Member, IEEE*

***Abstract*—Combined harnessing of electrical and thermal energies could leverage their complementary nature, inspiring the integration of power grids and centralized heating systems in future smart cities. This paper considers interconnected power distribution network (PDN) and district heating network (DHN) infrastructures through combined heat and power units and heat pumps. In the envisioned market framework, the DHN operator solves an optimal thermal flow problem given the nodal electricity prices and determines the best heat production strategy. Variate coefficients of performance of heat pumps with respect to different load levels are considered and modeled in a disciplined convex optimization format. A two-step hydraulic-thermal decomposition method is suggested to approximately solve the optimal thermal flow problem via a second-order cone program. Simultaneously, the PDN operator clears the distribution power market via an optimal power flow problem given the demands from the DHN. Electricity prices are revealed by dual variables at the optimal solution. The whole problem gives rise to a Nash-type game between the two systems. A best-response decentralized algorithm is proposed to identify the optimal operation schedule of the coupled infrastructure, which interprets a market equilibrium as neither system has an incentive to alter their strategies. Numeric results demonstrate the potential benefits of the proposed framework in terms of reducing wind curtailment and system operation cost.**

***Index Terms*—Decentralized operation, district heating network, market equilibrium, optimal thermal flow, optimal power flow, power distribution network, power-heat interdependence.**

## NOMENCLATURE

### *Abbreviations*

| | |
|---|---|
| ACOPF | Alternating current optimal power flow. |
| ADMM | Alternating direction method of multipliers. |
| CHP | Combined heat and power. |
| CLMP | Continuous locational marginal price. |
| COP | Coefficient of performance. |
| DHN | District heating network. |
| LMP | Locational marginal price. |
| OPF | Optimal power flow. |
| OTF | Optimal thermal flow. |
| PDN | Power distribution network. |
| SOCP | Second-order cone programming. |
| TES | Thermal energy storage. |

### *Sets*

| | |
|---|---|
| $S^B$ | Set of buses in PDN. |
| $S^L$ | Set of heat loads in DHN. |
| $S^{loop}$ | Set of loops in the DHN |
| $S^N$ | Set of nodes in DHN. |
| $S^P$ | Set of pipelines in DHN. |
| $S^S$ | Set of heat sources in DHN. |
| $S_i^{B,d}$ | Set of downstream buses connecting to bus $i$. |
| $S_i^{P,s}$ | Set of pipelines starting at node $i$. |
| $S_i^{P,e}$ | Set of pipelines ending at node $i$. |

### *Parameters*

| | |
|---|---|
| $C_p$ | Specific heat capacity of water. |
| $C_i^P$ | Capacity of heat pump. |
| $\text{COP}_i$ | Coefficient of performance of heat pump. |
| $h_{i,t}^L$ | Energy demand of heat loads. |
| $L_b$ | Length of pipeline. |
| $p_{i,t}^d/q_{i,t}^d$ | Active/reactive power demands. |
| $r_{ij}/x_{ij}$ | Line resistance/reactance. |
| $T_t^a$ | Ambient temperature at period $t$. |
| $\gamma_b$ | Coefficient of pressure loss in pipeline. |
| $\eta_i^c/\eta_i^d$ | Efficiencies of heat charge/discharge in TES units. |
| $\lambda_b$ | Heat transfer coefficient of pipeline. |
| $\mu_i^H$ | Thermal loss rate of TES unit. |
| $\rho^w$ | Contract price of renewable energy. |
| $\rho_P^H$ | The price of electricity sell, which could be either a constant or the LMP. |
| $\rho_H^P$ | The price of heat offered by CHP units in PDN. |
| $\Delta t$ | Duration of period. |

Manuscript received February 23, 2018; revised July 10, 2018 and September 11, 2018; accepted November 6, 2018. Date of publication November 14, 2018; date of current version August 21, 2019. This work was supported by the National Natural Science Foundation of China under Grant U1766203, Grant 51621065, and Grant 51807101. Paper no. TSG-00292-2018. *(Corresponding author: Shengwei Mei.)*

Y. Cao, W. Wei, and S. Mei are with the State Key Laboratory of Control and Simulation of Power System and Generation Equipment, Department of Electrical Engineering, Tsinghua University, Beijing 100084, China (e-mail: cao-y17@mails.tsinghua.edu.cn; wei-wei04@mails.tsinghua.edu.cn; meishengwei@tsinghua.edu.cn).

L. Wu is with the ECE Department, Stevens Institute of Technology, Hoboken, NJ 07030 USA (e-mail: lei.wu@stevens.edu).

M. Shahidehpour and Z. Li are with the Robert W. Galvin Center for Electricity Innovation, Illinois Institute of Technology, Chicago, IL 60616 USA (e-mail: ms@iit.edu; zhiyi.li@hawk.iit.edu).

Color versions of one or more of the figures in this paper are available online at http://ieeexplore.ieee.org.

Digital Object Identifier 10.1109/TSG.2018.2880909

*Decision Variables*

| | |
|---|---|
| $h^c_{i,t}/h^d_{i,t}$ | Charge/discharge rate of TES units. |
| $h^P_{i,t}$ | Thermal output of heat pump. |
| $h^S_{i,t}$ | Generation of heat source. |
| $l_{ij,t}/v_{i,t}$ | Square magnitude of line current/bus voltage. |
| $\text{LMP}_i$ | Locational marginal price or nodal price. |
| $\dot{m}^{p,s}_{b,t}/\dot{m}^{p,r}_{b,t}$ | Mass flow rate in supply/return pipeline. |
| $\dot{m}^S_{i,t}/\dot{m}^L_{i,t}$ | Mass flow rate of heat source/load. |
| $\Delta p^s_{b,t}/\Delta p^r_{b,t}$ | Pressure loss in supply/return pipeline. |
| $p_{i,t}/q_{i,t}$ | Nodal active/reactive power injection. |
| $P_{ij,t}/Q_{ij,t}$ | Active/reactive line power flow. |
| $p^g_{i,t}/p^w_{i,t}$ | Output of gas-fired generator/wind farm. |
| $p^{gD}_{i,t}/h^{gD}_{i,t}$ | Electric/thermal output of CHP unit in PDN. |
| $p^{gH}_{i,t}/h^{gH}_{i,t}$ | Electric/thermal output of CHP unit in DHN. |
| $w^H_{i,t}$ | Thermal energy stored in TES units. |
| $\tau r^{p,i}_{b,t}/\tau r^{p,o}_{b,t}$ | Temperature at inlet/outlet of return pipeline. |
| $\tau s^{p,i}_{b,t}/\tau s^{p,o}_{b,t}$ | Temperature at inlet/outlet of supply pipeline. |
| $\tau s^S_{i,t}/\tau r^S_{i,t}$ | Supply/return temperature of heat source. |
| $\tau s^L_{i,t}/\tau r^L_{i,t}$ | Supply/return temperature of heat load. |
| $\tau s^n_{i,t}/\tau r^n_{i,t}$ | Mixture temperature at supply/return node. |

## I. Introduction

ENERGY is the foundation of human society and modern life. Traditional fossil fuels have negative environmental impacts and limited reserves. Under the transition to a green and sustainable society, the mushrooming of renewable generations in power grids such as solar and wind power has been witnessed worldwide during the past decades [1]. However, renewable resources have not been fully utilized. In China, the curtailment of wind energy reached 33900 GWh and the curtailment rate was 15% in 2015 [2]. This is because large wind farms are located at northeast and northwest provinces, where the local electric power demands are relatively low, and long-distance delivery of volatile renewable power may impose great challenges on the system operation. Deploying energy storage facilities helps resolve the uncertainty issue, but remains a cost-intensive option. An up-to-date survey on different energy storage technologies and the pertinent costs can be found in [3].

In addition to managing energy production and consumption solely in the power system, the multi-carrier energy system [4]–[6] provides a new perspective on harnessing the complementary nature of heterogeneous energy resources more efficiently via energy system integration. In particular, electricity delivery possesses a high efficiency while thermal energy is easy to store. Furthermore, a large fraction of domestic electricity is utilized for producing heat in vast areas with long cold winters, such as north China and many European countries. These facts inspire the integration of an electric power grid and a heat supply network.

To unleash the synergy between electrical power and thermal energy, coordinated operation of power grids and heating systems becomes a hot topic in recent years [7], [8]. Actually, combined heat and power generation has already been an active research field for a long time. A centralized optimization method is proposed in [9] for managing heat and power productions with a detailed heat storage model; residential-level energy management of thermal and electrical appliances is studied in [10] and [11]. In above research, the network model of heating system is neglected. Considering pipeline model of district heating network (DHN) and heat transfer constraints, a general dispatch model for combined heat and power (CHP) units is investigated in [12] to exploit the flexibility of thermal system and reduce wind curtailment. Based on some specific network models, a multi-scale thermal storage model is proposed in [13] to reduce the primary energy consumption and improve the economy in district heating systems; optimal operation of DHN is investigated in [14] and [15] through reducing costs of pumping and heat loss. Systematic modeling of a DHN, a pipeline network delivering heat-conducting fluids, is comprehensively discussed in [16]. The formulation incorporates both hydraulic conditions and thermal conditions. The model in [16] has been further extended in [17] and [18] by incorporating temperature dynamics, based on which combined heat and power dispatch methods are proposed to exploit thermal storage capabilities of pipelines and building temperature control. A similar framework is employed in [19] to study unit commitment of the integrated heating and power system, and a two-stage robust optimization approach is adopted to cope with uncertain wind generation.

Most of aforementioned studies rely on a centralized optimization paradigm. In current practice, power systems and heating systems are managed by different entities, therefore, decentralized decision making is highly desired. To this end, a decentralized algorithm for combined heat and power dispatch is proposed in [20] based on Benders decomposition. At each iteration, either an optimality cut or a feasibility cut is sent to the power system operator according to the outcome of thermal flow calculation, while physical data of the two systems are kept private; no economic objective is pursued by the heating system. A consensus based decentralized algorithm is developed in [21], in which an alternating current optimal power flow (ACOPF) subproblem for the power system and a thermal flow optimization problem are solved alternatively. In the thermal flow model, the heating system is approximated by an equivalent circuit.

To the best of our knowledge, energy trading and market issues in the heat-power energy systems have not attracted much attention, and the reasons could be: i) thermal energy is usually charged at fixed prices in traditional heating systems, and there is not much economic benefit from improving production plans; ii) there is no clear market mechanism for energy trading between the power system and the heat system; iii) historically, coal-fired or gas-fired boilers are mainstream heating sources, and the synergy of the two systems is not prominent. However, the proliferation of CHP units and heat pumps has been greatly promoting the share of electricity consumption from heating devices in the total electricity demand, and intensifies the interaction between the two systems. Recent trends on power distribution system marketization [22] make it possible and profitable to realize market-driven energy transactions. Along this line, by extending the locational marginal price (LMP) scheme to DHN, a heat-power spot market is studied in [23], and the market equilibrium condition is

formulated as a mixed-integer linear program; strategic bidding of energy hub in heat-power market is discussed in [24] and comes down to a mathematical program with equilibrium constraints.

This paper focuses on multi-period operation of interconnected power distribution network (PDN) and DHN. The contribution is twofold.

1) We propose a two-step hydraulic-thermal decomposition algorithm to solve the nonlinear and nonconvex optimal thermal flow (OTF) model efficiently. In the OTF model, dynamic changes of heat pump coefficient of performance (COP) with respect to different load levels are considered, and the heat pump cost is formulated in line with a disciplined convex optimization format. Based on the loss analysis of pipelines, we propose a heuristic method to determine proper hydraulic conditions in DHN, as such the OTF gives rise to a convex program. The proposed method can find a near global solution very efficiently.

2) We propose a decentralized operation scheme for interdependent PDN and DHN by leveraging the distribution power market and time-varying nodal electricity prices. In the proposed framework, PDN and DHN can be independently operated by respectively solving an optimal power flow (OPF) problem and an OTF problem, given the status of the other network. The LMP is extracted from the dual variables associated with an exact nonlinear OPF model. System-level interaction is reflected by the fact that heat generation schedule changes the electricity demand, which will further impact LMPs; LMPs in turn influence the schedule of heat generation. The interaction is captured by a Nash-type game; however, dual variables do not appear in traditional Nash game models. A best-response algorithm is proposed to identify the market equilibrium state, at which neither system is willing to alter their strategies. A tailored continuous LMP (CLMP) scheme is developed to improve convergence performance and enhance market stability. Unlike the prevalent alternating direction method of multipliers (ADMM) for distributed optimization, the proposed algorithm is parameter-free and enjoys fast convergence due to the adoption of CLMP.

Compared with [23] which aims to discuss market impacts of elastic demands, no heat market exists in this paper. The branch flow model is also employed in [23], while its linearization depends on the special forms of two objective functions; moreover, even if the equilibrium conditions can be applied to the multi-period market in this paper, there would be a large number of complementarity and slackness conditions which quickly go beyond the capability of existing solvers. In this paper, we propose an iterative algorithm which involves solving tractable second-order cone programs (SOCPs). A tailored continuous LMP (CLMP) scheme is suggested to enhance market stability.

This paper is different from [24] in three aspects. (i) From the market structure, the market in [24] contains two levels; the energy hub strategically bids offering prices and quantities in the upper level, while the heating market and the power market in the lower level are connected to the energy hub but not directly connected to each other. In this paper, the PDN and the DHN connect to each other directly, and there is no intermediate agent. Both situations can happen, depending on the system structure and market organization. (ii) From the mathematical formulation, the linearized branch flow model is used in [24], and LMP is not involved; the bidding problem comes down to a bilevel program. In this paper, the exact power flow model is adopted, and electricity transaction follows LMPs; the market boils down to a single-level Nash-type game. (iii) From the solution method, the bilevel model in [24] is reformulated as a mixed-integer linear program, while the market equilibrium in this paper is solved by an iterative algorithm.

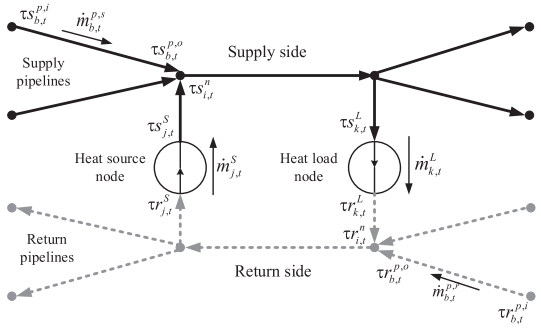


Fig. 1. Structure of the DHN.

The rest of this paper is organized as follows. The OTF problem and its two-step decomposition algorithm are introduced in Section II; the OPF problem and distribution power market clearing are described in Section III; the bilateral electricity and heating market structure and the decentralized operation scheme are set forth in Section IV; case studies are presented in Section V; finally, conclusions are summarized in Section VI.

## II. The OTF Problem

### A. Exact Formulation

A DHN consists of symmetric supply and return pipelines, and Fig. 1 shows the typical topology of a DHN. At each source (load) node, heat is injected into (withdrawn from) the network via a heat exchanger between the supply side and the return side. The network model is subject to hydraulic conditions and thermal conditions [16].

Hydraulic conditions describe the mass flow and fluid pressure in pipelines, which consist of the following formula:

*1) Continuity of Mass Flow:* For each node in the DHN, the mass flows entering the node are equal to the mass flows leaving the node.

$$\sum_{b\in S_i^{P,e}} \dot{m}_{b,t}^{p,s} + \sum_{j\in S_i^S} \dot{m}_{j,t}^S = \sum_{b\in S_i^{P,s}} \dot{m}_{b,t}^{p,s} + \sum_{k\in S_i^L} \dot{m}_{k,t}^L \tag{1}$$

$$\sum_{b\in S_i^{P,s}} \dot{m}_{b,t}^{p,r} + \sum_{k\in S_i^L} \dot{m}_{k,t}^L = \sum_{b\in S_i^{P,e}} \dot{m}_{b,t}^{p,r} + \sum_{j\in S_i^S} \dot{m}_{j,t}^S. \tag{2}$$

*2) Fluid Pressure Balance:* Due to the friction of pipelines, the fluid pressure decreases along the pipe, and the pressure loss is expressed as follows:

$$\Delta p_{b,t}^s = \gamma_b \left(\dot{m}_{b,t}^{p,s}\right)^2, \Delta p_{b,t}^r = \gamma_b \left(\dot{m}_{b,t}^{p,r}\right)^2 \tag{3}$$

According to the principle of pressure balance, the pressure loss in a closed loop is equal to zero.

$$\sum_{b\in S^{loop}} K_b \Delta p^s_{b,t} = 0, \ \sum_{b\in S^{loop}} K_b \Delta p^r_{b,t} = 0 \tag{4}$$

where $K_b = 1$ indicates that the direction of mass flow in pipeline $b$ is consistent with the loop direction; $K_b = -1$ indicates that the direction of mass flow in pipeline $b$ is opposite to the loop direction.

Thermal conditions characterize relations among nodal temperatures and thermal energy production/consumption, and consist of the following formula:

*3) Heat Source Model:* Thermal energy provided by heat sources is expressed as follows:

$$h^S_{i,t} = c_p \dot{m}^S_{i,t}(\tau s^S_{i,t} - \tau r^S_{i,t}) \tag{5}$$

Two kinds of heat sources are considered, which are CHP units and heat pumps. A CHP unit produces electricity and heat at the same time. This paper considers a general situation that some CHP units are operated by PDN (CHP-PDN for short), and others are operated by DHN (CHP-DHN for short). We do not consider third-party owned CHP units. Such profit-driven entity has been discussed in [24].

The feasible operation region of an extraction-condensing CHP unit is normally a polytope [25]. The operation cost of CHP-DHN is a bi-variate convex quadratic function in its electricity and heat outputs:

$$\begin{aligned} C^{GH}_{i,t} = {} & a^0_i + a^1_i p^{gH}_{i,t} + a^2_i h^{gH}_{i,t} \\ & + a^3_i (p^{gH}_{i,t})^2 + a^4_i (h^{gH}_{i,t})^2 + a^5_i p^{gH}_{i,t} h^{gH}_{i,t} \end{aligned} \tag{6}$$

According to the study in [26], the COP of a heat pump decreases with the increase in its output. We can approximate this relation via a decreasing linear function

$$\mathrm{COP}_i = -a\left(h^P_{i,t}/C^P_i\right) + b \tag{7}$$

In addition, heat pumps purchase electricity from PDN at the LMP, so its operation cost is given as:

$$C^{PH}_{i,t} = \mathrm{LMP}_i h^P_{i,t}/\mathrm{COP}_i \tag{8}$$

The DHN operator can buy heat from CHP-PDN units with a contract price, and the corresponding cost is:

$$C^{GD}_{i,t} = \rho^P_H h^{gD}_{i,t}. \tag{9}$$

*4) TES Unit Model:* Some heat pumps are equipped with thermal energy storage (TES) units. When electricity is cheaper, more heat can be produced and stored for future use. The storage dynamics in a TES unit is expressed as follows:

$$w^H_{i,t+1} = w^H_{i,t}\left(1-\mu^H_i\right) + \left(h^c_{i,t}\eta^c_i - h^d_{i,t}/\eta^d_i\right)\Delta t. \tag{10}$$

*5) Heat Load Model:* Heat consumption at a load node is:

$$h^L_{i,t} = c_p \dot{m}^L_{i,t}\left(\tau s^L_{i,t} - \tau r^L_{i,t}\right). \tag{11}$$

*6) Pipeline Model:* Due to inevitable heat loss, the temperature of fluid in pipelines drops along flow directions. The relation between inlet and outlet temperatures of each pipeline is established as:

$$\tau s^{p,o}_{b,t} = \left(\tau s^{p,i}_{b,t} - T^a_t\right) e^{-\frac{\lambda_b L_b}{C_p \dot{m}^{p,s}_{b,t}}} + T^a_t \tag{12}$$

$$\tau r^{p,o}_{b,t} = \left(\tau r^{p,i}_{b,t} - T^a_t\right) e^{-\frac{\lambda_b L_b}{C_p \dot{m}^{p,r}_{b,t}}} + T^a_t. \tag{13}$$

*7) Temperature at Confluence Nodes:* According to the energy conservation law, when fluids with different temperatures come across at a confluence node, the temperature of the mixture is calculated as:

$$\begin{aligned} & \sum_{b\in S^{P,e}_i}\left(\tau s^{p,o}_{b,t}\dot{m}^{p,s}_{b,t}\right) + \sum_{j\in S^S_i}\left(\tau s^S_{j,t}\dot{m}^S_{j,t}\right) \\ & \qquad = \tau s^n_{i,t}\left(\sum_{b\in S^{P,e}_i}\dot{m}^{p,s}_{b,t} + \sum_{j\in S^S_i}\dot{m}^S_{j,t}\right) \end{aligned} \tag{14}$$

$$\begin{aligned} & \sum_{b\in S^{P,s}_i}\left(\tau r^{p,o}_{b,t}\dot{m}^{p,r}_{b,t}\right) + \sum_{k\in S^L_i}\left(\tau r^L_{k,t}\dot{m}^L_{k,t}\right) \\ & \qquad = \tau r^n_{i,t}\left(\sum_{b\in S^{P,s}_i}\dot{m}^{p,r}_{b,t} + \sum_{k\in S^L_i}\dot{m}^L_{k,t}\right) \end{aligned} \tag{15}$$

In addition, the temperatures of leaving mass flows are equal to the temperature during mixing at the node.

$$\tau s^{p,i}_{b,t} = \tau s^n_{i,t}, \ \tau s^L_{k,t} = \tau s^n_{i,t} \tag{16}$$

$$\tau r^{p,i}_{b,t} = \tau r^n_{i,t}, \ \tau r^S_{j,t} = \tau r^n_{i,t} \tag{17}$$

Let $m^h$ be mass flow variables and $x^h$ all other decision variables of the DHN operator, then the OTF problem can be formulated as follows:

$$\begin{aligned} \min \quad & f_{OTF}(x^h) \\ \text{s.t.} \quad & \text{Hydraulic constraints (1)-(4)} \\ & \text{Thermal constraints (5), (10)-(17)} \\ & x^h_L \le x^h \le x^h_M, \ m^h_L \le m^h \le m^h_M \end{aligned} \tag{18}$$

where $x^h_L$ ($x^h_M$) and $m^h_L$ ($m^h_M$) are the lower (upper) bounds of $x^h$ and $m^h$, respectively. The objective function

$$f_{OTF} = \sum_t \left(\sum_i C^{GH}_{i,t} + \sum_j C^{PH}_{j,t} + \sum_k C^{GD}_{k,t}\right) \tag{19}$$

is comprised of operation costs of CHP-DHN units and heat pumps, as well as the payment for purchasing heat from the PDN. OTF problem (18) is non-convex due to the fractional cost function of heat pumps, products of mass flow and temperature variables in constraints (5), (11), (14), and (15), as well as exponential functions in constraints (12) and (13).

### B. An SOCP Approximation

*1) Convexifying the Objective Function:* The cost function of heat pumps could be written in the following form:

$$C_{i,t}^{PH} = \frac{\mathrm{LMP}_i h_{i,t}^P}{\mathrm{COP}_i} = \frac{b\mathrm{LMP}_i \left(C_i^P\right)^2}{a\left(bC_i^P - ah_{i,t}^P\right)} - \frac{\mathrm{LMP}_i C_i^P}{a} \tag{20}$$

whose second-order derivative is

$$\frac{\partial^2 C_{i,t}^{PH}}{\partial \left(h_{i,t}^P\right)^2} = \frac{2ab\mathrm{LMP}_i \left(C_i^P\right)^2}{\left(bC_i^P - ah_{i,t}^P\right)^3} > 0, \ \forall h_{i,t}^P \in \left[0, C_i^P\right] \tag{21}$$

implying the convexity of heat pump cost function in its entire feasible operation region. To state (20) in a disciplined convex form, we omit the second term of $C_{i,t}^{PH}$ in (20), which is a constant because LMP is fixed in OTF; then replace the first term with an axillary variable $\sigma_{i,t}$, and include the following inequalities in the constraints of the OTF problem:

$$\left\| \begin{matrix} 2\sqrt{\frac{b\mathrm{LMP}_i (C_i^P)^2}{a}} \\ \sigma_{i,t} - (bC_i^P - ah_{i,t}^P) \end{matrix} \right\|_2 \leq \sigma_{i,t} + \left(bC_i^P - ah_{i,t}^P\right) \tag{22}$$

$$\sigma_{i,t} \geq 0, \ h_{i,t}^P \geq 0, \ bC_i^P - ah_{i,t}^P \geq 0 \tag{23}$$

where (22) is a canonical second-order cone and (23) represents a polyhedral set, both of which are compatible with SOCP solvers. In fact, (22) and (23) are equivalent to

$$\sigma \geq \frac{b\mathrm{LMP}_i (C_i^P)^2}{a(bC_i^P - ah_{i,t}^P)}, \ bC_i^P - ah_{i,t}^P \geq 0 \tag{24}$$

So we actually performed an epigraph transformation [27]. Please note that inequality $bC_i^P - ah_{i,t}^P \geq 0$ does not affect heat pump operation, because it is a natural consequence of $\mathrm{COP}_i > 0$ according to (7). Compared with constant COP which leads to a linear cost function, (24) introduces only one second-order cone constraint and a linear inequality; other OTF constraints remain the same. So the problem size does not change much. It is revealed in [28] and [29] that the primal-dual interior-point algorithm has $O(\sqrt{n})$ iteration-complexity for both SOCP and LP, where $n$ denotes the number of constraints, implying that considering varying COP increases model accuracy while brings little extra computational burden.

*2) Approximating the Constraints:* It is observed that when mass flow variables are fixed, thermal constraints in the OTF problem (18) become linearized. Next we present a method to determine near-optimal mass flow rates based on network loss analysis. The rationale rests on the energy conservation law: the total heat production must be equal to the heat demand plus pipeline losses. As the demand is fixed, one natural way to cut down the cost is to reduce the losses.

The heat loss in a pipeline is expressed as follows:

$$\Delta Q_t^b = C_p \dot{m}_{b,t}^p \left(\tau_{b,t}^{p,i} - \tau_{b,t}^{p,o}\right) \tag{25}$$

Substituting equation (12) into equation (25) results in:

$$\Delta Q_t^b = C_p \dot{m}_{b,t}^p \left[\left(\tau_{b,t}^{p,i} - T_t^a\right)\left(1 - e^{-\frac{\lambda_b L_b}{C_p \dot{m}_{b,t}^p}}\right)\right] \tag{26}$$

**Algorithm 1** Two-Step Hydraulic-Thermal Decomposition

1: Set all the temperatures of pipelines to the lower limits and calculate the heat loss according to equation (27).
2: Optimize production plans of heat sources; the total output is equal to the summation of heat loads and pipeline losses.
3: Calculate nodal mass flow rates ($\dot{m}_{j,t}^S, \dot{m}_{k,t}^L$) according to (5) and (11) using the heat source outputs and heat loads.
4: Calculate mass flow rates ($\dot{m}_{b,t}^p$) in pipelines according to (1)-(4) using nodal mass flow rates ($\dot{m}_{j,t}^S, \dot{m}_{k,t}^L$).
5: Fix mass flow variables at $m_0^h$ obtained above, and solve the following problem

$$\begin{aligned} \min \quad & f_{OTF}(x^h) \text{ with given LMP} \\ \text{s.t.} \quad & (5),(10)\text{-}(17),(22)\text{-}(23) \text{ with } m^h = m_0^h \\ & x_L^h \leq x^h \leq x_M^h \end{aligned} \tag{28}$$

where $0 < \lambda_b L_b / C_p \dot{m}_{b,t}^p \ll 1$. Since $e^{-x} \approx 1 - x$, we have:

$$\Delta Q_t^b \approx C_p \dot{m}_{b,t}^p \left(\tau_{b,t}^{p,i} - T_t^a\right) \frac{\lambda_b L_b}{C_p \dot{m}_{b,t}^p} = \lambda_b L_b \left(\tau_{b,t}^{p,i} - T_t^a\right) \tag{27}$$

Equation (27) suggests that $\Delta Q_t^b$ is independent of mass flow rate $\dot{m}_{b,t}^p$. Recently, this phenomenon has been corroborated by experiments on real heating systems [30]. The sole controllable variable that influences $\Delta Q_t^b$ is the inlet temperature. In order to cut down the heat loss and reduce the operation cost, the overall operating temperature of the DHN should be controlled as low as possible. According to [16], the temperature lower limits of supply and return sides could be set as 70°C and 30°C, respectively.

Fixing mass flow variables, problem (18) renders a convex optimization problem. A two-step hydraulic-thermal decomposition method is suggested to find a near-optimal solution. The flowchart is summarized in Algorithm 1. In each single period, hydraulic conditions are determined first and remains unchanged, and then nodal temperatures are calculated according to the demands; from a multi-period perspective, the OTF formulation interprets a variable-flow variable-temperature operation. More exactly, in different time periods, the mass flow rates are adjustable in response to the variation of demands, and the temperatures only change slightly near their lower bounds. The advantage of this paradigm is that the mass flow rate, a mechanical variable, can change quickly by operating the circulating pump, while the temperature dynamics have large inertial due to the large specific heat capacity of water.

The proposed method is applied to the single-period OTF problem of a 10-node meshed DHN; its topology is shown in Fig. 2(a). System data are provided in [31]. We randomly generate 50 load scenarios, where the total demand varies from 3MW to 6MW. The exact model (18) is solved by Baron, a global solver for nonlinear programs; the optimal value is denoted as Opt-Glo; the convex approximation model (29) is solved by CPLEX; the optimal value is denoted as Opt-Apr. Since certain variables are fixed in (29), Opt-Apr $\geq$ Opt-Glo always holds. The optimality gap (Opt-Apr−Opt-Glo)/Opt-Glo is shown in Fig. 2(b). The gap has an order of magnitude

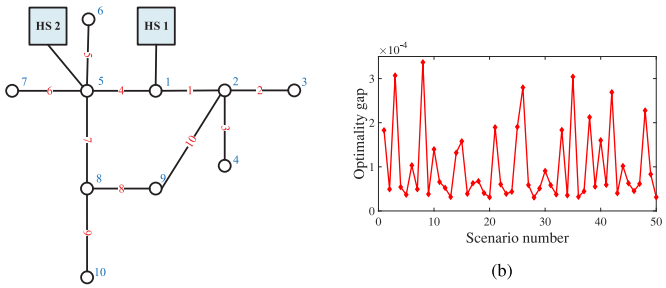


Fig. 2. (a) Topology of a 10-node DHN. (b) Optimality gap.

TABLE I
CALCULATION RESULTS OF MASS FLOW RATES ($kg/s$)

| Pipeline | Minimum Load | | | Average Load | | | Maximum Load | | |
|---|---|---|---|---|---|---|---|---|---|
| | Al | Baron | Error | A1 | Baron | Error | A1 | Baron | Error |
| 1 | 7.39 | 7.33 | 0.82% | 10.55 | 10.53 | 0.21% | 13.91 | 13.90 | 0.17% |
| 2 | 3.24 | 3.20 | 1.78% | 4.61 | 4.58 | 0.62% | 6.05 | 6.03 | 0.36% |
| 3 | 3.12 | 3.08 | 1.45% | 4.43 | 4.41 | 0.40% | 5.82 | 5.81 | 0.20% |
| 4 | 0.65 | 0.66 | 3.07% | 1.27 | 1.25 | 0.91% | 1.93 | 1.95 | 1.02% |
| 5 | 3.00 | 2.98 | 0.75% | 4.26 | 4.23 | 0.53% | 5.59 | 5.56 | 0.45% |
| 6 | 3.12 | 3.23 | 3.48% | 4.43 | 4.50 | 1.56% | 5.82 | 5.86 | 0.68% |
| 7 | 5.23 | 5.21 | 0.42% | 7.35 | 7.36 | 0.04% | 9.61 | 9.60 | 0.14% |
| 8 | 2.04 | 2.02 | 1.38% | 2.83 | 2.83 | 0.10% | 3.67 | 3.67 | 0.11% |
| 9 | 3.19 | 3.19 | 0.18% | 4.52 | 4.53 | 0.13% | 5.94 | 5.94 | 0.10% |
| 10 | 1.02 | 1.06 | 3.95% | 1.51 | 1.54 | 1.57% | 2.03 | 2.05 | 0.99% |

of $10^{-4}$ in all 50 instances, indicating that Algorithm 1 offers high-quality OTF solutions. The average computation times of Baron and Algorithm 1 are 1357s and 1.14s, respectively. The default tolerance of optimal value gap of Baron is $10^{-6}$. If we change it to $10^{-4}$, the computation time is 1043s, still much longer than the proposed method.

Mass flow rates of individual pipelines in the minimum, average, and maximum demand scenarios are summarized and compared in Table I (where A1 is abbreviation for Algorithm 1). The relative error of optimal solution is also very small, and decreases with the increase in loads. According to previous analysis, the larger the value of $\dot{m}$, the smaller the value of $x$, and the more concise the approximation made in (27). Experiments conducted in [30] suggest that in most cases, (27) is satisfactory if the mass flow rate is greater than 1kg/s.

Furthermore, we test a 24-period OTF problem by incorporating time-varying heat demand across a day. In this test, Baron fails to converge after running for 5 hours, while Algorithm 1 finds a solution in 9.87s. The speedup of Algorithm 1 mainly benefits from its convex programming formulation of OTF problem with fixed mass flow rates, which is based on the property of heat loss revealed in (27). We also test IPOPT, a local solver for nonlinear programs, and the average solver time for the 24-period OTF problem is 96s.

It should be pointed out that the water flow in a DHN is maintained by a circulating pump, which consumes certain amount of electricity. In normal conditions, the energy consumed by the circulating pump is far less than a heat pump, so the cost of circulating pump is negligible in the OTF problem.

## III. THE OPF PROBLEM

We envision an distribution power market which is cleared via an OPF problem, charging consumers at the LMP. Because a PDN is usually operated with a tree topology, the power flow equations can be described by the branch flow model [32].

$$p_{j,t} = \sum_{k \in S_j^{B,d}} P_{jk,t} - \left(P_{ij,t} - r_{ij} l_{ij,t}\right) + p_{i,t}^d \tag{29}$$

$$q_{j,t} = \sum_{k \in S_j^{B,d}} Q_{jk,t} - \left(Q_{ij,t} - x_{ij} l_{ij,t}\right) + q_{i,t}^d \tag{30}$$

$$v_{j,t} = v_{i,t} - 2\left(r_{ij} p_{ij,t} + x_{ij} q_{ij,t}\right) + \left(r_{ij}^2 + x_{ij}^2\right) l_{ij,t} \tag{31}$$

$$l_{ij,t} v_{i,t} = P_{ij,t}^2 + Q_{ij,t}^2 \tag{32}$$

where $p_{j,t}$ denotes the total active power injection at bus $j$, in period $t$, including the output of gas-fired generators, CHP unit, and wind farm. The generator at the slack bus mimics the power supplied from the transmission network. The total cost of PDN includes four components described in (33)-(36). The operating cost of a CHP-PDN unit is a bi-variate convex quadratic function in electricity and heat generations:

$$C_{i,t}^{GD} = b_i^0 + b_i^1 p_{i,t}^{gD} + b_i^2 h_{i,t}^{gD} + b_i^3 \left(p_{i,t}^{gD}\right)^2 + b_i^4 \left(h_{i,t}^{gD}\right)^2 + b_i^5 p_{i,t}^{gD} h_{i,t}^{gD} \tag{33}$$

The operation cost of a gas-fired generator is modeled by a univariate convex quadratic function:

$$C_{i,t}^{PT} = c_i^0 + c_i^1 p_{i,t}^g + c_i^2 \left(p_{i,t}^g\right)^2 \tag{34}$$

Electricity can be purchased from CHP-DHN units, and the payment is:

$$C_{i,t}^{HP} = \rho_P^H p_{i,t}^{gH} \tag{35}$$

where $\rho_H^P$ denotes the trading price of electricity; it could be a fixed contract price or the LMP. If the latter is adopted, we fix $\rho_P^H$ at the LMP obtained in the last iteration.

Wind farms provide cheap electricity at a fixed contract price, and the corresponding cost is:

$$C_{i,t}^{WP} = \rho^w p_{i,t}^w \tag{36}$$

The total operating cost of PDN is given by

$$f_{OPF} = \sum_t \left( \sum_i C_{i,t}^{GD} + \sum_j C_{j,t}^{PT} + \sum_k C_{k,t}^{HP} + \sum_s C_{s,t}^{WP} \right)$$

Let $x^d$ be a vector of decision variables of the PDN, so that security boundary constraints can be represented by

$$x_L^d \le x^d \le x_M^d \tag{37}$$

Expressing line capacity constraints in the form of

$$\sqrt{P_{ij,t}^2 + Q_{ij,t}^2} \le S_{ij} \tag{38}$$

will not jeopardize the convexity of (37).

It is revealed that constraint (32) which is non-convex can be replaced by a rotated second-order cone [32]

$$l_{ij,t}v_{i,t} \geq P_{ij,t}^2 + Q_{ij,t}^2 \tag{39}$$

and (39) naturally holds as an equality at the optimal solution of the OPF problem. In this way, the OPF problem can be represented as an SOCP

$$\begin{aligned} \min \quad & f_{OPF} \\ \text{s.t.} \quad & \text{Cons-PF with given DHN demands} \\ & (37),\ (38) \end{aligned} \tag{40}$$

where Cons-PF contains (29)-(31) and (39). In case that the convex relaxation in (39) is not exact, the sequential SOCP approach in [33] can be applied to recover the optimal solution, because the distance between the inexact solution and feasible/optimal solutions to the original OPF problem is usually very small. This approach has been generalized in [34] to cope with OPF problems over meshed power grids.

After OPF problem (40) is solved, nodal electricity prices, also known as LMPs, can be retrieved from the Lagrangian dual multipliers associated with nodal active power balance equalities (29). The procedure of solving OPF and calculating LMP is called distribution market clearing.

We do not model uncertainty of wind generation in the OPF problem. The reason is that in heat-power integrated systems discussed in this paper, wind spillage is mainly caused by its opposite tendency compared to the electric load curve, which will be illustrated through case studies.

## IV. The Market Driven Approach

### A. Market Settings

Heat and electricity transactions between the PDN and the DHN obey the following rules:

1) CHP units owned by the PDN can sell heat to DHN at a contract price $\rho_H^P$. The quantity is bid by DHN.
2) CHP units owned by the DHN can sell electric power to PDN at price $\rho_P^H$, which could be either a constant or the LMP; the latter is adopted in this paper. The quantity is bid by PDN.
3) Heat pumps purchase electricity at LMP.

The market structure is summarized in Fig. 3. One larruping feature of the proposed framework is the LMP based electricity transaction. As industrial heat pumps and CHP units possess considerably larger capacities than residential appliances, they have the potential to influence market prices, which makes the decision making more complicated: on the one hand, when the DHN operator performs the OTF and determines heat production plans, LMPs are needed as input; on the other hand, when the PDN operator conducts the OPF and clears the distribution market, electricity demands of heat pumps are needed as input. This interaction precipitates a Nash-type game and outcomes a market equilibrium in the integrated system.

### B. An Algorithm for Decentralized System Operation

In the proposed decentralized operation method, the DHN operator solves the OTF with fixed boundary variables, i.e., LMPs and electric power output of CHP-DHN units, and then submits heat pump power demands and heat requests from CHP-PDN units to the power grid; the PDN operator clears the market with fixed power and heat requests from the DHN, updates LMPs and power demands from PDN-DHN units, and then sends them to the heating system. The iterative procedure continues until certain convergence tolerance is met. The basic steps have been summarized in Algorithm 2.

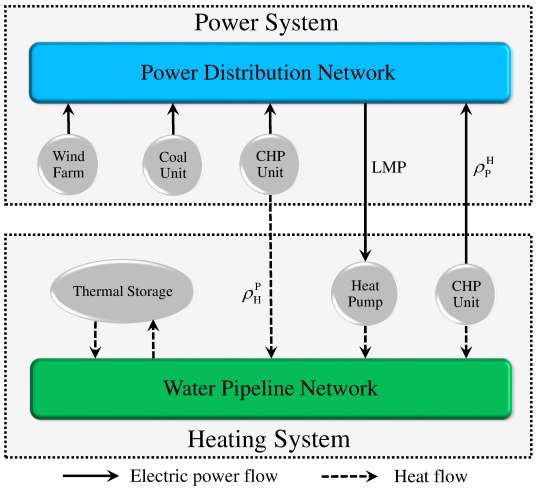


Fig. 3. Market structure of the integrated system.

**Algorithm 2** Best-Response Decentralized Algorithm

1: Set a tolerance $\varepsilon > 0$ and a maximum number of iterations $N^{max}$. All variables are initialized as $\mathbf{x}^0 = 0$, including heat pump power demands; LMPs are initiated as the marginal cost of the largest generator at rated output. The iteration index is set as $n = 0$.
2: Solve OPF problem (40) with fixed demands from the DHN and $\rho_P^H$ being the LMP at corresponding bus in last iteration, record the optimal solution in $\mathbf{x}^{n+1}$, and retrieve LMPs. Send LMPs and power demands to the DHN.
3: Solve OTF problem (18) with fixed LMPs and demands from the PDN, record the optimal solution in $\mathbf{x}^{n+1}$, then send both power and heat demands to the PDN.
4: If $|\mathbf{x}^{(n+1)} - \mathbf{x}^{(n)}| < \varepsilon$, terminate and report $\mathbf{x}^{(n+1)}$ as the final result; else if $n > N^{max}$, quit and report that the algorithm fails to converge; else update $n \leftarrow n+1$ and go to step 2.

More dedicated initialization in step 1 can accelerate convergence. Step 2 and step 3 are interchangeable, depending on the available information. For example, if the DHN operator could forecast LMP from historical data and statistic analysis, then the OTF problem can be solved first in step 2.

Because the objective function of OTF involves LMPs, the dual variables of OPF, it is not trivial to mathematically prove the convergence condition of Algorithm 2. In our study, we observe that when a heat pump is installed at a downstream bus of a wind farm, the output of this heat pump may fail to converge in the iterative procedure and oscillation may occur. The phenomenon is analyzed as follows. Consider a heat pump

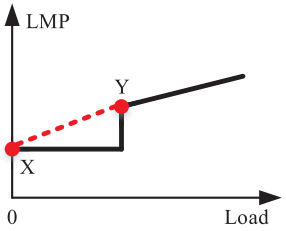


Fig. 4. Illustration of CLMP.

and its corresponding LMP. In a certain iteration, it consumes little electricity and surplus wind generation is curtailed at the upstream bus, then LMP will be close to the wind power offering price $\rho^w$ which is low. Hence, the heat pump will increase its output at this iteration; as a result, wind power is no longer curtailed, and the LMP may witness a sudden rise. At the next iteration, the heat pump will opt to decrease its output and the LMP may return to the wind power offering price. In this way, oscillation takes place due to the discontinuity of LMP.

A CLMP method is suggested in [35] to circumvent the disadvantage of the traditional LMP scheme. Basically, it uses a continuous piecewise linear function to approximate the discontinuous LMP-demand curve. CLMP is adopted at electric buses where LMPs are not continuous. The solid black line in Fig. 4(a) shows the traditional LMP as a function of electric load. In this paper, the step point is mainly caused by wind power spillage, so a tailored CLMP scheme is suggested as follows.

1) At a heat pump connected bus, set the power consumed by heat pump to zero and solve the OPF problem. The calculated LMP is represented by X;
2) Increase the power consumed by heat pump until no wind power is curtailed and solve the OPF problem. The calculated LMP is representd by Y.
3) CLMP curve is represented by the red dashed line connecting X and Y.

In this way, at the PDN side, LMPs are increasing with the growth of heat pump demands according to OPF results; at the DHN side, the heat pump demands are decreasing with the rise of LMPs according to OTF results. The intersection of price and demand curves interprets the market equilibrium.

## V. Case Studies

### A. System Configurations

A testing heat-power integrated energy system composed of an IEEE 33-bus PDN and a 32-node DHN modified from [16] is used to demonstrate the performance of the proposed method. System topology is shown in Fig. 5. Energy production facilities include 3 gas-fired generators, 2 wind farms, 1 CHP-PDN unit, 1 CHP-DHN unit and 3 heat pumps. TES units located at nodes 5, 18, 24 in the DHN are not shown in Fig. 5. Power and heat load profiles, and forecasted maximum wind generation outputs are shown in Fig. 6. We can see that the heat demand has a tendency opposite to the power load curve but consistent with wind generation. Complete system data

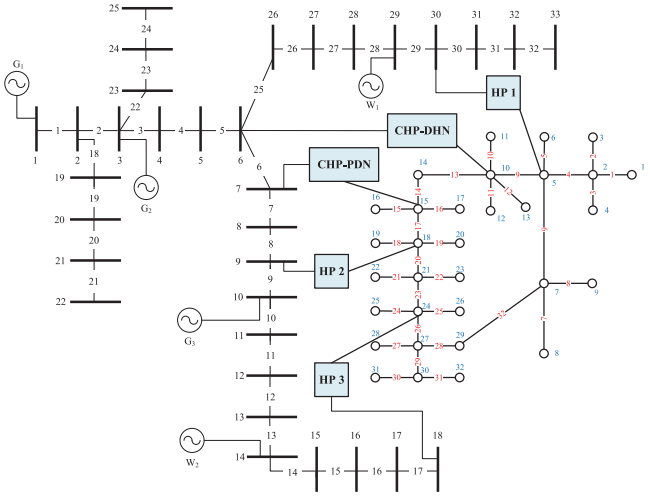


Fig. 5. Topology of the integrated system.

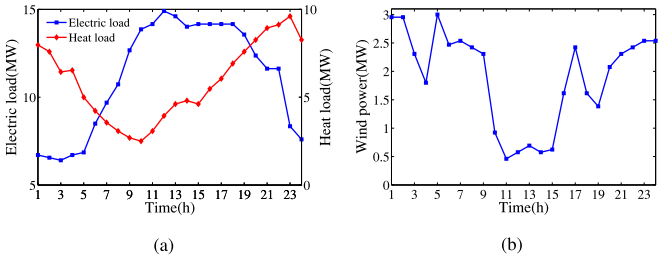


(a) (b)

Fig. 6. (a) Electric and heat loads. (b) Wind power forecast.

are provided in [31]. All experiments are conducted on a laptop with Intel i5-7300HQ CPU and 8G memory. Optimization models are solved by CPLEX.

### B. Analysis of CLMP Scheme

In the benchmark case, Algorithm 2 without CLMP scheme is tested first. Fig. 7(a) shows the incremental output of heat pump #1 between two successive iterations in period 5, and Fig. 7(b) gives the LMP at bus 30. As analyzed in Section IV, persistent oscillations are observed. Then the CLMP scheme is applied, results are provided in Fig. 7(c) and Fig. 7(d). We can see that Algorithm 2 converges successfully after 9 iterations.

The spatial and temporal variation of LMPs in the PDN is portrayed in Fig. 8a. In the temporal horizon, we can see that the LMP curves at individual buses follow similar tendency: higher during daytime and lower across night periods because of the difference of load levels. In the spatial horizon, the slice at period 12 is shown in Fig. 8b. Clearly, LMP increases along the power flow direction. The LMP at bus 7 is the lowest because a CHP unit of low marginal cost is connected to this bus.

### C. Comparison of Mark-Oper and Cont-Oper

As a comparison, a pure contract-based situation is considered, in which heat pump power consumptions are paid at a constant contract price. The network operation is decoupled: the DHN operator solves the OTF first and submits electricity demands to the PDN, and then the PDN operator solves

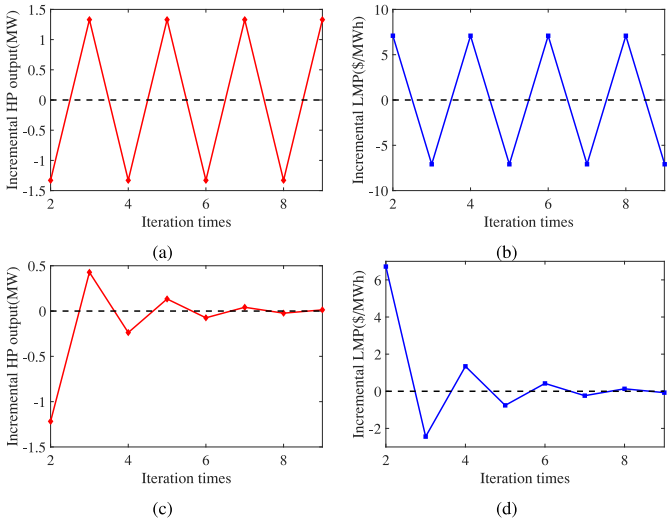


Fig. 7. Incremental values between two successive iterations: (a) output of HP1 without CLMP method ; (b) LMP at bus 30 without CLMP method; (c) output of HP1 with CLMP method; (d) LMP at bus 30 with CLMP method.

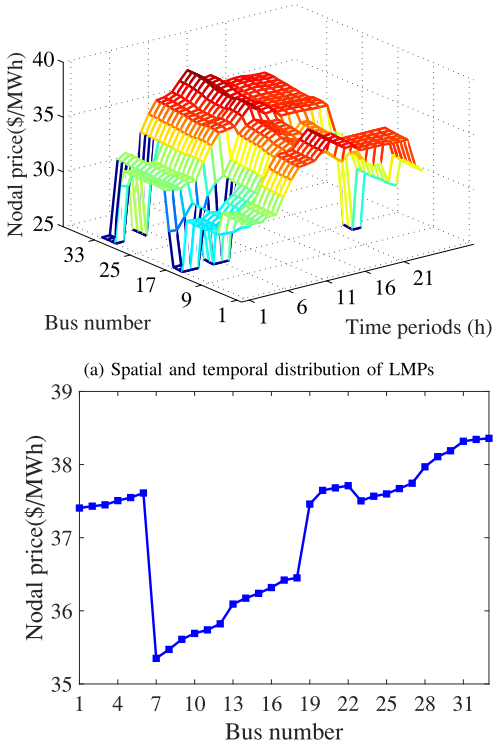


Fig. 8. System LMPs.

the OPF and determines power dispatch. The market based scheme is termed as Mark-Oper, and the contract-based one is referred to as Cont-Oper.

Assuming the contract price in Cont-Oper mode is the daily average LMP 34$/MWh, the dispatched wind power in two schemes are compared in Fig. 9(a). In general, wind power curtailment occurs during the night owing to low electric loads and high wind power outputs. In addition, because the electricity price is flat and heat pumps have less incentive to buy excessive wind power for heat production. For Mark-Oper

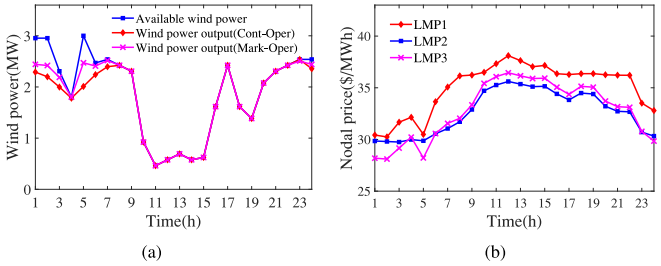


Fig. 9. (a) Wind power usage. (b) LMPs related to HPs in Mark-Oper scheme.

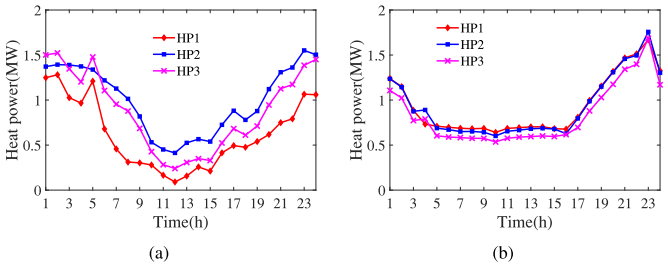


Fig. 10. Output of HPs in (a) Mark-Oper scheme. (b) Cont-Oper scheme.

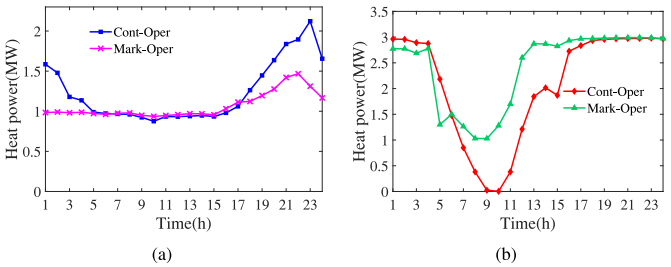


Fig. 11. (a) Heat produced by CHP unit in DHN. (b) Heat produced by CHP unit in PDN.

scheme, LMPs at heat pump connection buses are shown in Fig. 9(b). When the wind power is abundant, the LMP is low, encouraging the use of surplus wind power during night which can be observed from Fig. 9(a) and heat pump output curves in Fig. 10.

The daily operation costs of DHN under Mark-Oper and Cont-Oper schemes are $2428 and $2698, respectively. Heat produced by CHP units is depicted in Fig. 11. The generation cost of CHP-DHN units are quadratic functions of heat generation, and the marginal costs increase with the increasing of heat generation. The heat produced by CHP-DHN units in Mark-Oper scheme is always lower than that in Cont-Oper scheme, as power to heat conversion enabled by heat pumps enjoys a lower marginal cost than CHP-DHN unit, which demonstrates the superiority of the market-driven framework. In addition, when the LMP is high at daytime in Mark-Oper, heat pump will consume less electricity compared to that in Cont-Oper. Therefore, DHN operators tend to purchase more heat from CHP-PDN units to supply the demand at daytime in Mark-Oper.

Storage dynamics in both schemes are shown in Fig. 12. In Mark-Oper scheme, TES units are charged in periods 1-11 when electricity is cheap and begin to discharged at period 17

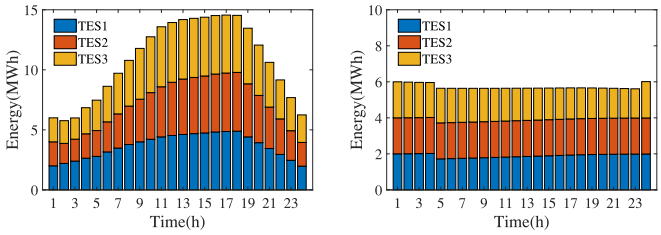


Fig. 12. Storage dynamics in (a) Mark-Oper scheme. (b) Cont-Oper scheme.

TABLE II
RESULTS WITH RESPECT TO DIFFERENT CONTRACT PRICES

| Contract price ($/MWh) | 32 | 33 | 34 | 35 | 36 |
|---|---|---|---|---|---|
| Spillage (%) | 6.02 | 6.64 | 7.23 | 7.92 | 8.54 |
| DHN cost ($) | 2631 | 2667 | 2698 | 2723 | 2742 |
| PDN cost ($) | 8896 | 8874 | 8853 | 8836 | 8822 |
| Total cost ($) | 11527 | 11541 | 11551 | 11559 | 11564 |

when electricity price is high and heat load starts to grow; during periods 11-16, the heat demand is low, so the storage levels do not change much. These observations are consistent with the outputs of heat pumps shown in Fig. 10. Compared with Cont-Oper scheme, TES units have deeper charging and discharging levels in Mark-Oper, which help flatten the electricity load profile by shaving peaks and filling valleys. Thus, Mark-Oper scheme driven by time-varying LMPs benefits both power and heat systems.

### D. Impact of Contract Price

We investigate the impact of the contract price in Cont-Oper on the curtailment rates and operation costs. Results are listed in Table II. The wind power spillage grows with the increase in contract price, because heat pumps tend to purchase less electricity due to the higher price. The DHN operation cost increases at the same time, but even when the contract price is 32$/MWh, the economy is still worse than that in Mark-Oper. PDN operation cost decreases because of the reduction in power consumptions of head pumps.

### E. Impact of Wind Penetration Level

We investigate the performance of the proposed method under different levels of wind power generations. We multiply the wind power forecast in Fig. 6b with a scale ratio varying from 0.6 to 1.4. The numbers of iterations, wind curtailment rates and operation costs in both Mark-Oper and Cont-Oper are listed in Table III. The curtailment rate grows with the increase in wind generation in both Mark-Oper and Cont-Oper. Owing to the increase of wind power, both electricity price and DHN operation cost in Mark-Oper decrease. On the contrary, DHN operation cost remains the same because of the fixed electricity price in Cont-Oper. PDN operation cost decreases in both schemes because of the increasing use of wind power. In general, Algorithm 2 takes more iterations to converge when more wind power is available, because LMPs in more periods become discontinuous. Nevertheless, with the help of CLMP, Algorithm 2 still converges successfully.

TABLE III
RESULTS WITH RESPECT TO DIFFERENT WIND POWER LEVELS

| Wind power Ratio | | 0.6 | 0.8 | 1.0 | 1.2 | 1.4 |
|---|---|---|---|---|---|---|
| Mark-Oper | Iterations | 5 | 6 | 9 | 21 | 17 |
| | Spillage (%) | 0 | 1.02 | 4.18 | 7.51 | 12.83 |
| | DHN cost ($) | 2594 | 2523 | 2428 | 2352 | 2282 |
| | PDN cost ($) | 9103 | 9014 | 8967 | 8912 | 8872 |
| | Total cost ($) | 11697 | 11537 | 11395 | 11264 | 11154 |
| Cont-Oper | Spillage (%) | 0.21 | 2.52 | 7.23 | 12.95 | 18.97 |
| | DHN cost ($) | 2698 | 2698 | 2698 | 2698 | 2698 |
| | PDN cost ($) | 8997 | 8914 | 8853 | 8803 | 8764 |
| | Total cost ($) | 11695 | 11612 | 11551 | 11501 | 11462 |

TABLE IV
RESULTS WITH DIFFERENT WIND SCENARIOS

| | Maximum | Minimum | Mean | Standard deviation |
|---|---|---|---|---|
| Spillage (%) | 6.05 | 2.60 | 4.34 | 0.77 |
| DHN cost ($) | 2463 | 2402 | 2430 | 13.57 |
| PDN cost ($) | 8980 | 8953 | 8968 | 6.40 |
| Total cost ($) | 11443 | 11355 | 11398 | 18.02 |

### F. Economic Impact of Wind Volatility

In the coupled heat-power energy system studied in this paper, volatility will not be a major cause of wind curtailment, and wind power spillage is mainly triggered by its opposite tendency compared to the electric load curve, which can be observed from Fig. 6.

Nevertheless, wind uncertainty will impact system daily operation economy. To investigate this effect, we assume that wind power forecast error obeys Gaussian distribution with zero mean, and the standard deviation is 0.1 multiplying the forecast values. We generate 1000 wind generation scenarios and execute Algorithm 2 under each scenario. The statistical performance of curtailment rates and operation costs are listed in Table IV. The standard deviation of DHN operation cost, PDN operation cost and total operation cost are about 0.5%, 0.07% and 0.16% of their respective mean values.

### G. Impact of Heat Pump Capacity

Finally, we investigate the impact of heat pump capacity on the performance of the proposed model. We adjust their capacities by multiplying $C_i^P$ with a scale ratio varying from 0.6 to 1.4. Results are listed in Table V. With the increase in heat pump capacity, the wind curtailment rate decreases gradually. Since bigger heat pump capacities may cause larger incremental changes of boundary variables in two consecutive steps, the number of iterations increases consequently. In addition, larger heat pump has a higher efficiency with the same load level according to (7). Therefore, DHN operation cost decreases with the increase in heat pump capacity in both Mark-Oper and Cont-Oper. PDN operation cost increases because more power is consumed by heat pumps.

TABLE V
RESULTS WITH DIFFERENT HEAT PUMP CAPACITIES

| Capacity Ratio | | 0.6 | 0.8 | 1.0 | 1.2 | 1.4 |
|---|---|---|---|---|---|---|
| Mark-Oper | Iterations | 5 | 8 | 9 | 12 | 14 |
| | Spillage (%) | 5.49 | 5.21 | 4.18 | 3.23 | 2.43 |
| | DHN cost ($) | 2456 | 2435 | 2428 | 2412 | 2403 |
| | PDN cost ($) | 8951 | 8963 | 8967 | 8971 | 8973 |
| | Total cost ($) | 11407 | 11398 | 11395 | 11383 | 11376 |
| Cont-Oper | Spillage (%) | 8.45 | 7.85 | 7.23 | 6.79 | 6.40 |
| | DHN cost ($) | 2705 | 2701 | 2698 | 2694 | 2691 |
| | PDN cost ($) | 8843 | 8848 | 8853 | 8857 | 8861 |
| | Total cost ($) | 11548 | 11549 | 11551 | 11551 | 11552 |

## VI. CONCLUSION

In this paper, we propose a decentralized market framework for energy transaction in the interdependent PDN and DHN based on distribution power market and LMP. Combing a convex approximation for the OTF problem and a convex relaxation for the OPF problem, we develop a convex optimization based decomposition algorithm for decentralized system operation in the market environment. Oscillation phenomenon caused by the discontinuity of ordinary LMP scheme is analyzed, and a CLMP scheme is employed to improve the convergence performance and facilitate the design of a more stable market. Case studies show that compared with a contract based energy trading at a fixed price, the proposed market framework not only allows the optimal system operation, but also creates additional opportunities of spatial and temporal demand response that flattens the load profile via real-time electricity prices. In-depth theoretical study on the existence and characteristics of the market equilibrium as well as new trading schemes such as sharing energy markets will be the focuses of our future work.

## REFERENCES


[1] X. Yang, Y. Song, G. Wang, and W. Wang, "A comprehensive review on the development of sustainable energy strategy and implementation in China," *IEEE Trans. Sustain. Energy*, vol. 1, no. 2, pp. 57–65, Jul. 2010.

[2] A Global Wind Energy Council. (2016). *Global Wind Report 2015*. [Online]. Available: http://www.gwec.net/wp-content/uploads/vip/GWEC-Global-Wind-2015-Report_April-2016_22_04.pdf

[3] L. Yao *et al.*, "Challenges and progresses of energy storage technology and its application in power systems," *J. Mod. Power Syst. Clean Energy*, vol. 4, no. 4, pp. 519–528, Oct. 2016.

[4] M. Geidl and G. Andersson, "Optimal power flow of multiple energy carriers," *IEEE Trans. Power Syst.*, vol. 22, no. 1, pp. 145–155, Feb. 2007.

[5] M. Geidl *et al.*, "Energy hubs for the future," *IEEE Power Energy Mag.*, vol. 5, no. 1, pp. 24–30, Jan./Feb. 2007.

[6] X. Zhang, M. Shahidehpour, A. Alabdulwahab, and A. Abusorrah, "Optimal expansion planning of energy hub with multiple energy infrastructures," *IEEE Trans. Smart Grid*, vol. 6, no. 5, pp. 2302–2311, Sep. 2015.

[7] N. Good and P. Mancarella, "Flexibility in multi-energy communities with electrical and thermal storage: A stochastic, robust approach for multi-service demand response," *IEEE Trans. Smart Grid*, to be published.

[8] T. Sun, J. Lu, Z. Li, D. Lubkeman, and N. Lu, "Modeling combined heat and power systems for microgrid applications," *IEEE Trans. Smart Grid*, vol. 9, no. 5, pp. 4172–4180, Sep. 2018.

[9] X. Chen *et al.*, "Increasing the flexibility of combined heat and power for wind power integration in China: Modeling and implications," *IEEE Trans. Power Syst.*, vol. 30, no. 4, pp. 1848–1857, Jul. 2015.

[10] G. Belli *et al.*, "A unified model for the optimal management of electrical and thermal equipment of a prosumer in a DR environment," *IEEE Trans. Smart Grid*, to be published.

[11] N. Neyestani, M. Yazdani-Damavandi, M. Shafie-Khah, G. Chicco, and J. Catalão, "Stochastic modeling of multienergy carriers dependencies in smart local networks with distributed energy resources," *IEEE Trans. Smart Grid*, vol. 6, no. 4, pp. 1748–1762, Jul. 2015.

[12] Y. Dai *et al.*, "Dispatch model for CHP with pipeline and building thermal energy storage considering heat transfer process," *IEEE Trans. Sustain. Energy*, to be published.

[13] V. Verda and F. Colella, "Primary energy savings through thermal storage in district heating networks," *Energy*, vol. 36, no. 7, pp. 4278–4286, Jul. 2011.

[14] P. Jie, N. Zhu, and D. Li, "Operation optimization of existing district heating systems," *Appl. Therm. Eng.*, vol. 78, pp. 278–288, Mar. 2015.

[15] E. Guelpa *et al.*, "Optimal operation of large district heating networks through fast fluid-dynamic simulation," *Energy*, vol. 102, pp. 586–595, May 2016.

[16] X. Liu, J. Wu, N. Jenkins, and A. Bagdanavicius, "Combined analysis of electricity and heat networks," *Appl. Energy*, vol. 162, pp. 1238–1250, Jan. 2016.

[17] Z. Li, W. Wu, M. Shahidehpour, J. Wang, and B. Zhang, "Combined heat and power dispatch considering pipeline energy storage of district heating network," *IEEE Trans. Sustain. Energy*, vol. 7, no. 1, pp. 12–22, Jan. 2016.

[18] C. Wu *et al.*, "Combined economic dispatch considering the time-delay of district heating network and multi-regional indoor temperature control," *IEEE Trans. Sustain. Energy*, vol. 9, no. 1, pp. 118–127, Jan. 2018.

[19] Z. Li, W. Wu, J. Wang, B. Zhang, and T. Zheng, "Transmission-constrained unit commitment considering combined electricity and district heating networks," *IEEE Trans. Sustain. Energy*, vol. 7, no. 2, pp. 480–492, Apr. 2016.

[20] C. Lin, W. Wu, B. Zhang, and Y. Sun, "Decentralized solution for combined heat and power dispatch through benders decomposition," *IEEE Trans. Sustain. Energy*, vol. 8, no. 4, pp. 1361–1372, Oct. 2017.

[21] J. Li, J. Fang, Q. Zeng, and Z. Chen, "Optimal operation of the integrated electrical and heating systems to accommodate the intermittent renewable sources," *Appl. Energy*, vol. 167, pp. 244–254, Apr. 2016.

[22] Y. Liu, J. Li, and L. Wu, "Distribution system restructuring: Distribution LMP via unbalanced ACOPF," *IEEE Trans. Smart Grid*, vol. 9, no. 5, pp. 4038–4048, Sep. 2018.

[23] Y. Chen, W. Wei, F. Liu, E. Sauma, and S. Mei, "Energy trading and market equilibrium in integrated heat-power distribution systems," *IEEE Trans. Smart Grid*, to be published.

[24] R. Li, W. Wei, S. Mei, Q. Hu, and Q. Wu, "Participation of an energy hub in electricity and heat distribution markets: An MPEC approach," *IEEE Trans. Smart Grid*, to be published.

[25] T. Guo, M. I. Henwood, and M. Van Ooijen, "An algorithm for combined heat and power economic dispatch," *IEEE Trans. Power Syst.*, vol. 11, no. 4, pp. 1778–1784, Nov. 1996.

[26] E. Bilgen and H. Takahashi, "Exergy analysis and experimental study of heat pump systems," *Exergy Int. J.*, vol. 2, no. 4, pp. 259–265, May 2002.

[27] S. P. Boyd and L. Vandenberghe, *Convex Optimization*. Cambridge, U.K.: Cambridge Univ. Press, 2004.

[28] R. D. C. Monteiro and I. Adler, "Interior path following primal-dual algorithms. Part I: Linear programming," *Math. Program.*, vol. 44, nos. 1–3, pp. 27–41, May 1989.

[29] R. D. C. Monteiro and T. Tsuchiya, "Polynomial convergence of primal-dual algorithms for the second-order cone program based on the MZ-family of directions," *Math. Program.*, vol. 88, no. 1, pp. 61–83, Jun. 2000.

[30] B. van der Heijde, A. Aertgeerts, and L. Helsen, "Modelling steady-state thermal behaviour of double thermal network pipes," *Int. J. Therm. Sci.*, vol. 117, pp. 316–327, Jul. 2017.

[31] (2018). *Integrated System Data*. [Online]. Available: https://sites.google.com/site/caoyangthu13/data

[32] M. Farivar and S. H. Low, "Branch flow model: Relaxations and convexification—Part I," *IEEE Trans. Power Syst.*, vol. 28, no. 3, pp. 2554–2572, Aug. 2013.

[33] W. Wei, J. Wang, N. Li, and S. Mei, "Optimal power flow of radial networks and its variations: A sequential convex optimization approach," *IEEE Trans. Smart Grid*, vol. 8, no. 6, pp. 2974–2987, Nov. 2017.

[34] Z. Tian and W. Wu, "Recover feasible solutions for SOCP relaxation of optimal power flow problems in mesh networks," *arXiv preprint 1708.06504*, 2017.

[35] F. Li, "Continuous locational marginal pricing (CLMP)," *IEEE Trans. Power Syst.*, vol. 22, no. 4, pp. 1638–1646, Nov. 2007.

**Yang Cao** (S'18) received the B.Sc. degree in electrical engineering from Tsinghua University, Beijing, China, in 2017, where he is currently pursuing the Ph.D. degree.

His research interest includes planning and operation of multicarrier energy systems.

**Wei Wei** (M'15–SM'18) received the Bachelor and Ph.D. degrees in electrical engineering from Tsinghua University, Beijing, China, in 2008 and 2013, respectively.

He was a Post-Doctoral Research Associate with Tsinghua University from 2013 to 2015. He was a Visiting Scholar with Cornell University, Ithaca, NY, USA, in 2014 and Harvard University, Cambridge, MA, USA, in 2015. He is currently an Assistant Professor with Tsinghua University. His research interests include applied optimization and energy system economics.

**Lei Wu** (SM'13) received the B.S. degree in electrical engineering and the M.S. degree in systems engineering from Xi'an Jiaotong University, Xi'an, China, in 2001 and 2004, respectively, and the Ph.D. degree in electrical engineering from the Illinois Institute of Technology (IIT), Chicago, IL, USA, in 2008.

He was a Senior Research Associate with the Robert W. Galvin Center for Electricity Innovation, IIT, from 2008 to 2010. He was a Visiting Faculty with NYISO in 2012. He was a Professor with the Electrical and Computer Engineering Department, Clarkson University, Potsdam, NY, USA, in 2018. He is currently an Associate Professor with the Electrical and Computer Engineering Department, Stevens Institute of Technology, Hoboken, NJ, USA. His research interests include power systems operation and planning, energy economics, and community resilience microgrid.

**Shengwei Mei** (F'15) received the B.Sc. degree in mathematics from Xinjiang University, Urumqi, China, in 1984, the M.Sc. degree in operations research from Tsinghua University, Beijing, China, in 1989, and the Ph.D. degree in automatic control from the Chinese Academy of Sciences, Beijing, in 1996.

He is currently a Professor with Tsinghua University. His research interests include power system complexity and control, game theory and its application in power systems.

**Mohammad Shahidehpour** (F'01) received the Honorary Doctorate degree from the Polytechnic University of Bucharest, Bucharest, Romania, in 1981.

He is a University Distinguished Professor, the Bodine Chair Professor, and the Director of the Robert W. Galvin Center for Electricity Innovation, Illinois Institute of Technology. He serves as the Editor-in-Chief for the *Journal of the Modern Power Systems and Clean Energy*. He is a member of the U.S. National Academy of Engineering and a fellow of the American Association for the Advancement of Science and the National Academy of Inventors.

**Zhiyi Li** (S'14–M'17) received the B.S. degree in electrical engineering from Xi'an Jiaotong University, Xi'an, China, in 2011, the M.S. degree in electrical engineering from Zhejiang University, China, in 2014, and the Ph.D. degree from the Electrical and Computer Engineering Department, Illinois Institute of Technology, Chicago, IL, USA, in 2017.

He is currently a Visiting Faculty with the Robert W. Galvin Center for Electricity Innovation, Illinois Institute of Technology.